Yield Shear Strength Ratio for Liquefaction Triggering Analysis of Tailings Dams

I.A. Contreras, PhD, PE
Barr Engineering Co., Minneapolis, MN, USA
B.E. Zwissler, PhD
Barr Engineering Co., Minneapolis, MN, USA

ABSTRACT: Liquefaction is one of the most common causes of catastrophic failure of tailings dams, challenging engineers to assess liquefaction potential and develop designs to account for both static and dynamic triggers. Liquefaction analysis includes the evaluation of liquefaction triggering, which typically incorporates yield shear strength ratio, $s_{u \text{ (yield)}}/\sigma'_{vo}$. A common procedure for estimating $s_{u \text{ (yield)}}/\sigma'_{vo}$ uses cone penetration test (CPT) data in the form of normalized cone penetration resistance, q_{c1}, or standard penetration test (SPT) data in the form of normalized blow-count, $(N_1)_{60}$. This paper presents a preliminary relationship for the estimation of s_u (yield) σ'_{vo} from CPT as a function of the equivalent clean sand cone penetration resistance, Q m,cs. This is believed to be a better parameter than qc1 when assessing the strength of fine-grained materials (i.e., fine tailings) because it accounts for tip resistance, sleeve friction, and pore-water pressure. The relationship was developed by combining s_u (yield) σ'_{vo} from the case history database developed by Olson and Stark (2003) and the corresponding $Q_{in,cs}$ reported by Robertson (2010). The relationship also includes data collected by the authors at a tailings basin using CPT (for Q m,cs) and vane shear tests (FVT) (for s_u (yield)/ σ'_{vo}) conducted in adjacent soundings at the same depths. The preliminary relationship shows relatively good agreement between the $s_{u \text{ (yield)}}/\sigma'_{vo}$ from the case history database and the authors' fine tailings dataset, but requires a more robust dataset covering a wider range of Q m,cs and soil behavior types (SBT) to enhance the relationship and better establish the trend between Q $_{tn,cs}$ and $s_{u \text{ (yield)}}/\sigma'_{vo}$.

1 INTRODUCTION

Because many mine tailings impoundments involve structures constructed with or on top of saturated soils deposited in a loose condition, soil liquefaction is a major design concern. Liquefaction occurs in undrained conditions and is induced by static or dynamic loading. Liquefaction is characterized by a sudden decrease in shear strength from the yield strength to the steady-state strength, which can be substantially lower. The loss of shear strength during liquefaction is so significant that the soil temporarily acts like a thick liquid (Terzaghi et al. 1996). At mine tailings impoundments, the consequences of liquefaction can include flow slides of sloping ground, lateral displacement of dams and retaining structures, ground rupture, formation of sand boils, and catastrophic failure of tailings dams.

Even though fine tailings contain significant amounts of silt- and clay-size particles, they are often susceptible to liquefaction because they typically contain low plasticity or non-plastic solids. The potential for fine tailings to liquefy in response to triggering events is related to the fact that these materials are often hydraulically deposited, come to equilibrium under loose conditions, and tend to remain continually saturated. Furthermore, liquefaction is typically observed in young, natural soil deposits like fine tailings, which are a waste material from mining processing operations (i.e., deposits of a fairly young geologic age). The loose condition resulting from the deposition method and the young age of fine tailings generally results in contractive behavior during undrained shearing.

Liquefaction analysis of slopes, embankments, and sloping foundations represents a challenge for engineers because of the complex nature of this assessment. In general, the analysis involves three steps: (1) a liquefaction susceptibility analysis, (2) a liquefaction triggering analysis, and (3) a post-triggering/flow failure stability analysis.

In the first step (<u>liquefaction susceptibility analysis</u>), engineers determine whether the material is contractive or dilative. Contractive material is susceptible to liquefaction and strain softening, while dilative material is not. Researchers have developed several relationships using CPT and SPT data with laboratory test results that distinguish between contractive and dilative sandy materials.

If the material is found to be contractive, the second step (<u>liquefaction triggering analysis</u>) is performed to determine if liquefaction will be triggered. This is done by determining whether the anticipated static shear stress or seismic stresses will exceed the yield shear strength of the contractive soils. In the case of seismic triggering, this step includes a site-response analysis that allows calculation of the factor of safety against triggering. This analysis requires the yield shear strength ratio s_u (yield)/ σ 'yo.

If it is determined that liquefaction will be triggered, the third step (post-triggering/flow failure stability analysis) is conducted to determine if the static shear forces are greater than the available shear resistance. If the factor of safety against flow failure, FS_{FLOW}, is less than or equal to unity, flow failure is predicted to occur once triggered. This analysis requires the liquefied shear strength ratio $s_{u \text{ (lig)}}/\sigma'_{vo}$.

This paper presents a relationship to estimate the yield shear strength ratio s_u (yield)/ σ 'vo for use in liquefaction triggering analysis. The proposed relationship uses CPT data ($Q_{m,cs}$) to estimate the yield shear strength ratio. The relationship was developed using two data sources: (a) the case history database published by Olson and Stark (2003) and augmented by Robertson (2010) and (b) data from adjacent CPT and FVT soundings in fine tailings from basins where the authors have worked. For the database of case histories, yield shear strengths were back-calculated from post-failure analyses and $Q_{m,cs}$ were measured from post-failure CPT soundings. For the fine tailings data collected by the authors, the yield shear strengths were measured from FVT soundings; $Q_{m,cs}$ were measured from adjacent CPT soundings at the same depths.

2 TRIGGERING LIQUEFACATION IN TAILINGS BASINS

Figure 1 illustrates the behavior of saturated, contractive, sandy soils during undrained shearing or loading (Olson and Stark 2003), applicable to fine tailings. Yield shear strength, $s_{u \text{ (yield)}}$, is the peak shear strength available to the soil during undrained loading (Terzaghi et al. 1996) and is illustrated as point B in Figure 1. In contrast, steady-state (or liquefied) shear strength, $s_{u \text{ (liq)}}$, illustrated as point C in Figure 1, becomes the shear strength available to the soil during and after undrained strain softening (or liquefaction) has occurred. Liquefaction can be triggered by both static and dynamic loads, as well as by deformation under static shear stress that exceeds the liquefied shear strength.

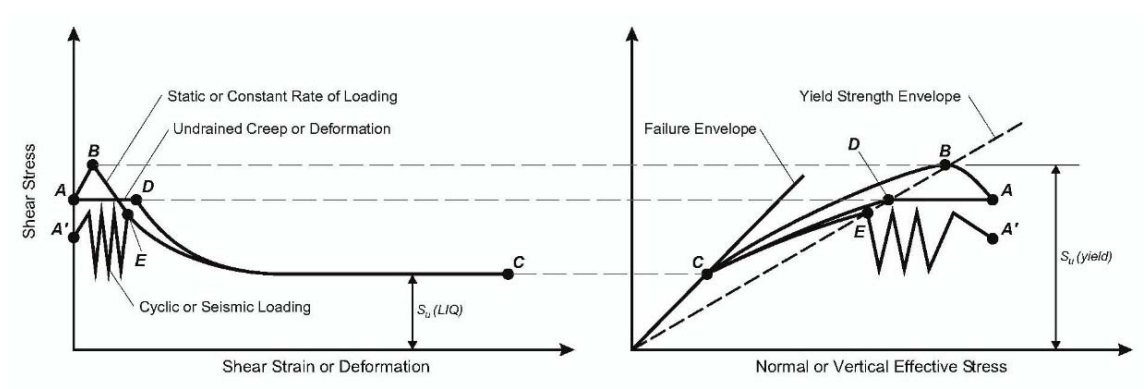


Figure 1. Undrained response of saturated contractive sandy soils, including fine tailings (after Olson and Stark 2003)

Liquefaction triggered by static or monotonic loading (illustrated by the yield shear strength envelope connecting Point A and Point B to Point C in Fig. 1) can occur at tailings impoundments during activities such as tailings deposition on a slope or upstream dam construction. For static liquefaction triggering to occur, the shear stress in the saturated fine tailings must exceed Point B during undrained conditions. Once triggered, the loose structure of the soil particles yield and collapse, causing the loss of shear strength with additional shear strain, illustrated as the curve between Point B and C. If enough shear strain is experienced by the soil to reach Point C, liquefied shear strength (Point C) governs the fine tailings.

Liquefaction triggered by deformation under static shear loading (illustrated by the yield shear strength envelope connecting Point A and Point D to Point C in Fig. 1) can also occur at tailings impoundments during events such as dam foundation deformation or erosion at the toe of a slope. For liquefaction to be triggered by static shear deformation, the static shear strain must exceed that at Point D and the effective stress must drop below that at Point D during undrained conditions. Once triggered, just as with liquefaction triggered by monotonic loading, the loosely packed soil particles yield and collapse, causing the loss of shear strength with additional shear strain, illustrated as the curve between Point D and C. If enough shear strain is experienced by the soil to reach Point C, liquefied shear strength (Point C) then governs the fine tailings.

Liquefaction triggered by seismic or dynamic loading (illustrated by the yield shear strength envelope connecting Point A and Point E to Point C in Fig. 1) can occur at tailings impoundments during earthquakes or be caused by vibrations from construction activities. For dynamic liquefaction to occur, the duration and intensity of the seismic/dynamic load must cause enough excess pore-water pressure within the fine tailings that the effective stress drops below that at Point E during undrained conditions. Once triggered, just as with static and deformation-induced liquefaction, the loosely packed soil particles yield and collapse, causing the loss of shear strength with additional shear strain, illustrated as the curve between Point E and C. If enough shear strain is experienced by the fine tailings to reach Point C, liquefied shear strength (Point C) governs.

Most liquefaction analysis discussions in literature are associated with liquefaction of sandy deposits during seismic events. However, mine tailings, which are typically fine-grained with low plasticity, have undergone more static than seismic liquefaction events (Davies et al. 1998). Tailings basins should be operated and constructed such that changes in load within the fine tailings are slow enough to prevent significant generation of excess pore-water pressures. In this case, the tailings are sheared under drained conditions during normal operation, avoiding static liquefaction. However, circumstances can occur at tailings basins that involve rapid changes in load or stress changes that can lead to localized undrained loading conditions, triggering static liquefaction. These shear stress changes can be caused by factors such as foundation deformation, erosion at the toe of a slope, change in piezometric head, or seismic shaking. Table 1 summarizes some typical triggering mechanisms associated with upstream tailings dams. The first four mechanisms are associated with monotonic (static) loading or deformation-induced liquefaction triggering. The fifth mechanism, acceleration and/or vibration, is associated with seismically or dynamically induced liquefaction triggering.

Liquefaction triggering analysis is a particularly important step in the assessment of tailings basins that uses the upstream construction method which has portions of the embankment dam founded on top of liquefiable materials (Contreras et al. 2016). As a result, there is a static shear stress applied to the fine tailings prior to a liquefaction triggering event. Table 1 also shows that some triggering events can be very small. This is why some research (Silvis and de Groot 1995, Robertson 2010) suggests that triggering should always be assumed if the soils are susceptible to strength loss. Details on conducting a liquefaction triggering analysis are discussed in the following section.

Table 1. Triggering Mechanisms for Liquefaction Failures of Upstream Tailings Dams (after Martin and McRoberts 1999)

Triggering Mechanism	Potential Cause
Over-steepening at toe	- Erosion (intense stormwater runoff, pipeline break causing washout)
	- Construction activities or "housekeeping" (excavation)
Overloading of slope/foundation	- Rapid rate of impoundment raising
	- Steepening of slope near crest
	- Construction activities at crest
Changes in pore pressures	- Seepage breakout on face of dam
	- Deterioration in performance of under drainage measures
	- Concentrated tailings discharge at one location for extended period
	- Accelerated rate of construction
	- Foundation or embankment movement
	- Intense rainstorms
	- Increased pond levels
Overtopping of dam	- Severe stormwater runoff
11 6	- Failure of diversion dams/ditches
	- Blockage and failure of spillways/decants
	- Embankment settlement/deformation and loss of freeboard
Acceleration/vibration	- Earthquakes
	- Construction traffic
	- Blasting

3 LIQUEFACATION TRIGGERING ANALYSIS

There are well-established procedures for liquefaction triggering analysis of level ground, including Seed et al. (1985) and Youd et al. (2001). However, there are few procedures to evaluate the triggering of liquefaction in sloping ground, including Poulos et al. (1985a), Seed and Harder (1990), and most recently Olson and Stark (2003). In the authors' opinion, Olson and Stark (2003) provide the most appropriate procedure for liquefaction triggering analysis of fine tailings on sloping ground, which is the basis of the liquefaction analysis discussion in this paper.

The Olson and Stark (2003) liquefaction triggering analysis procedure uses the yield undrained shear strength ratio, s_u (yield)/ σ'_{vo} , to evaluate the triggering of liquefaction in sloping ground subjected to static shear stress. The analysis procedure determines whether the combined static, seismic, and/or other shear stresses exceed the yield shear strength of the contractive material. This allows for the calculation of the factor of safety against liquefaction triggering. In this procedure, the yield shear strength ratio, s_u (yield)/ σ'_{vo} , is an important parameter required to assess liquefaction triggering. Olson and Stark (2003) proposed relationships to estimate this ratio, developed by back-analysis of case histories with SPT and CPT data available.

4 YIELD UNDRAINED SHEAR STRENGTH RATIO, $S_{U \text{ (YIELD)}}/\sigma'_{VO}$

The relationship proposed by Olson and Stark (2003) to estimate the yield shear strength ratio, $s_{u \text{ (liq)}}/\sigma'_{vo}$, uses the normalized cone tip resistance, q_{c1} . This relationship was developed by backanalyzing 33 case histories of liquefaction flow failures and correlating the yield shear strength ratio with the normalized cone tip resistance. Normalized cone tip resistance, q_{c1} , corrects CPT tip resistance for effective overburden stress, but does not use any correction for soil type, fines content, sleeve friction, or pore-water pressure. Olson and Stark (2003) advised that the relationship using CPT should be corrected for unequal end area effects through use of the corrected cone tip resistance, q_t .

Using the 33 case histories presented by Olson and Stark (2003) and adding three new cases where reliable CPT was available, Robertson (2010) introduced a CPT-based relationship to evaluate the susceptibility to strength loss and to predict the liquefied shear strength ratio, $s_{u \text{ (liq)}}/\sigma'_{vo}$. To use normalized CPT data to estimate liquefied shear strength ratio, $s_{u \text{ (liq)}}/\sigma'_{vo}$, Roberson (2010)

introduced the normalized equivalent clean sand cone resistance value, $Q_{m,cs}$. This corrects for effective overburden stress, soil type, and pore-water pressure. The normalized cone parameters are given by the following equations:

$$Q_{tn} = \left[\frac{q_t - \sigma_{vo}}{p_a}\right] \left(\frac{p_a}{\sigma'_{vo}}\right)^n \tag{1}$$

$$F_r = [f_s/(q_t - \sigma_{v0})] \times 100\%$$
 (2)

where q_t is the corrected cone resistance, p_a is the atmospheric pressure, and σ_{vo} and σ'_{vo} are total stress and effective stress, respectively. The exponent n is a function of the SBT index, I_c , which is defined by Equation 3:

$$I_{c} = [(3.47 - \log Q_{t})^{2} + (\log F_{r} + 1.22)2]^{0.5}$$
(3)

The stress exponent n in Equation 1 varies with both SBT index I_c (soil type) and stress level given by Equation 4:

$$n = 0.38(I_c) + 0.05 (\sigma'_{v0}/p_a) - 0.15$$
 where $n \le 1.0$ (4)

Finally, the normalized equivalent clean sand ($Q_{tn,cs}$) is given by Equation 5:

$$Q_{tn,cs} = K_c (Q_{tn}) \tag{5}$$

where K_c is a correction factor that is a function of the soils characteristics as follows:

$$K_c = 1.0$$
 if $I_c \le 1.64$
 $K_c = 5.581I_c^3 -0.403 I_c^4 -21.63 I_c^2 +33.75 I_c -17.88$ if $I_c > 1.64$ (6)

Robertson (2010) uses normalized equivalent clean sand cone resistance value, $Q_{tn,cs}$, to propose a boundary that separates contractive and dilative soil response and indicates that the contours of the equivalent clean sand cone resistance, $Q_{tn,cs}$, are essentially contours of the state parameter, ψ . Based on the work developed by Jefferies and Been (2006), who postulated that the boundary between contractive and dilative soil is related to a state parameter, ψ , of -0.05, Robertson proposed that a contour line of normalized equivalent clean sand cone resistance, $Q_{tn,cs}$, equal to 70 separates contractive and dilative soil response. Robertson (2010) also introduced a relationship that represents a lower bound estimate of the liquefied shear strength ratio, s_{u} (liq)/ σ 'vo, based on the normalized equivalent clean sand cone resistance, $Q_{tn,cs}$.

Robertson (2010) reports the normalized equivalent clean sand cone resistance, $Q_{ln,cs}$, for 33 case histories, and Olson and Stark (2003) report the yield strength ratio, s_u (yield)/ σ 'vo, for 29 case histories. Therefore, it is possible to combine the normalized equivalent clean sand cone resistance, $Q_{ln,cs}$, from Robertson (2010) with the corresponding yield strength ratio, s_u (yield)/ σ 'vo, from Olson and Stark (2003) to develop a relationship to estimate yield strength ratio, s_u (yield)/ σ 'vo, as a function of the normalized equivalent clean sand cone resistance, $Q_{ln,cs}$.

Such a relationship would be valuable for use in liquefaction triggering analysis for fine tailings. Many fine tailings are intermediate materials that cannot be classified simply as sand or silt or clay. This makes it difficult to obtain representative samples (Kramer and Wang 2015, Shuttle and Cunning 2007) for characterization with typical laboratory testing (Poulos et al. 1985a, Poulos et al. 1985b, Poulos 1988), which makes in-situ characterization appealing. Many existing in-situ correlations do not accurately represent the behavior of intermediate materials like fine tailings, but their behavior can be more accurately characterized by $Q_{tn,cs}$. This is because $Q_{tn,cs}$ accounts for tip resistance, sleeve friction, soil type, and pore-water pressure, which are all significant for fine tailings. Developing this relationship to estimate s_u (yield)/ σ 'vo as a function of $Q_{tn,cs}$ using the case history database was the starting point for this paper.

In addition to the case history database, the authors have accumulated extensive experience through work at tailings basins. A valuable data set has been developed by the authors in which adjacent CPT and FVT soundings have been conducted within fine tailings at a tailings impoundment. The FVT allows for direct measurement of the yield shear strength, and the CPT data allows for the calculation of the normalized equivalent clean sand cone resistance, $Q_{tn,cs}$. The following details the case history database and fine tailings dataset, which were used to develop the proposed correlation between s_{u} (yield)/ σ'_{vo} and $Q_{tn,cs}$.

4.1 Case histories data used in proposed relationship for yield shear strength ratio

Table 2 contains a summary of the case histories presented by Olson and Stark (2003) and augmented by Robertson (2010) that were used in this paper. For consistency, the case history numbers and structure names identified in Table 2 are the same used by Olson and Stark (2003) and Robertson (2010).

The classes reported in Table 2 are based on Robertson's (2010) classifications and serve as a way to represent the reliability of the data for each case history. Class A cases had reliable CPT measurements that included both tip resistance and sleeve friction values. Class B cases had less reliable CPT measurements and included mechanical or electric tip resistance values without sleeve friction values. Case histories where CPT values were estimated from either SPT, relative density, or best estimates were identified as Class C, Class D, or Class E, respectively, and were considered the least reliable. Similar to Robertson (2010), this paper only considered case histories with Class A and B data, since the data comes from actual CPT results and is considered reliable.

Approximate D_{50} and fines content (FC) for each case were reported by Olson and Stark (2003). Normalized cone resistance, Q_{tn} ; normalized friction ratio, F_r ; soil behavior type index, I_c ; and normalized equivalent clean sand cone resistance, $Q_{tn,cs}$, were reported for each case by Robertson (2010). These values are all summarized in Table 2.

Undrained yield shear strength ratio, s_u (yield)/ σ'_{vo} , was reported by Olson and Stark (2003) for many of the case histories shown in Table 2. However, for three cases, other sources were used to estimate the undrained yield shear strength ratio. For case 15, the undrained yield shear strength ratio was obtained from Olson (2001). For cases 9 and 27, the normalized cone resistance, q_{c1} , was obtained from Olson and Stark (2003). This was used to calculate brittleness index, I_B , and estimate yield undrained shear strength ratio, s_u (yield)/ σ'_{vo} , using methods from Sadrekarimi (2014).

In total, 10 case histories (categorized as class A or B with available $Q_{tn,cs}$ data and either reported yield shear strength ratio or supporting data to calculate it) were selected for use in the development of a relationship between s_u (yield)/ σ'_{vo} and $Q_{tn,cs}$, as summarized in Table 2.

Case history number ¹	Structure ¹	Class ²	Approx. D ₅₀ ¹ (mm)	Approx. FC ¹ (%)	Q_{tn}^2	F _r ² (%)	I_c^2	$Q_{tn,cs}^2$	Yield strength ratio ³
1	Zeeland	В	0.12	3 to 11	30	0.25	2.1	43	0.265
9	Kawagishi-Cho Bldg.	В	0.35	<5	31	0.5	2.2	50	0.283
14	Hokkaido Tails Dam	В	0.074	50	4	1.50	3.2	36	0.195
15	LSFD	A	0.074	50 (5-90)	5	3.5	3.3	52	0.282
17	Mochi-Koshi Tailings 1	В	0.04	85	5	2.5	3.3	48	0.27
18	Mochi-Koshi Tailings 2	В	0.04	85	5	2.5	3.3	48	0.22
19, 20, 21	Nerlerk Slide 1, 2, 3	A	0.22	2 to 12	40	0.4	2.0	55	0.21
22	Hachiro-Gata Road	В	0.2	10 to 20	30	0.5	2.2	50	0.16
27	Fraser River Delta	A	0.25	0 to 5	15	1.5	2.6	58	0.368
31	Soviet Tajik	В	0.012	100	19	1.0	2.6	53	0.30

Table 2. Case Histories of Flow Liquefaction Failures with Measured Penetration Resistance

4.2 Fine tailings data used in proposed relationship for yield shear strength ratio

Table 3 presents the fine tailings data collected by the authors where CPT soundings were performed adjacent to FVT soundings at 10 locations across a tailings basin. The testing was conducted in fine tailings with low plasticity (plasticity index typically less than 12 percent). The fine tailings tested at these 10 locations were found to have a soil behavior type (SBT) distribution as follows: 58% SBT 3, 19% SBT 4, 21% SBT 5, and 2% SBT 6. According to the classification provided by Robertson (1990), these SBT values correspond to "clays – clay to silty clay" (SBT 3), "silt mixtures – clayey silt to silty clay" (SBT 4), "sand mixtures – silty sand to sandy

⁽¹⁾ From Olson and Stark (2003)

⁽²⁾ From Robertson (2010)

⁽³⁾ Yield strength ratio for case 15 from Olson (2001) and for cases 9 and 27 calculated using Olson and Stark (2003) and Sadrekarimi (2014). All other yield strength ratios from Olson and Stark (2003).

silt" (SBT 5), and "sands – clean sands to silty sands" (SBT 6). The predominant materials in these deposits were characterized as clays, silt mixtures, and sand mixtures (SBT 3, 4, and 5), with clays and silt mixtures (SBT 3 and 4) accounting for 77% of the fine tailings.

FVT allows for direct in-situ measurement of the peak shear strength during undrained loading, which represents the yield shear strength, $s_{u \text{ (yield)}}$. FVT is the only in-situ testing method that provides a direct measurement of undrained shear strength. For the authors' tailings dataset (Table 3), FVT was conducted using electronic equipment that measures the torque down the hole at a rotation rate based on Blight (1968) to maintain undrained conditions during testing (Castro 2003).

Figure 2 shows that the FVT results compare well to the CPT interpretation of the undrained shear strength. Because CPT does not measure undrained shear strength directly, a site-specific bearing capacity factor, N_{kt}, of 16 was used to interpret the CPT shown in Figure 2.

Table 3. Tailings Locations with Adjacent CPT and Undrained Shear Strength (FVT) Measurements

Tailings location	Class 1	SBT ²	Q_{tn}^{3}	Fr ³ (%)	$I_c^{\ 3}$	$Q_{tn,cs}^{3}$	Yield strength ratio ⁴
A	A	3,4,5	5.62	1.06	2.99	37.3	0.339
В	A	3,4	4.39	1.44	3.14	37.1	0.258
C	A	3,4,5	4.75	1.50	3.12	38.7	0.329
D	A	3	3.66	2.07	3.29	38.5	0.287
E	A	3	3.91	1.23	3.16	34.0	0.215
F	A	3	3.68	1.11	3.17	32.3	0.200
G	A	3	5.18	1.44	3.08	39.7	0.252
Н	A	3,4	6.58	1.26	2.95	40.6	0.240
I	A	3	3.35	1.70	3.28	34.9	0.254
J	A	3	3.12	1.99	3.60	50.2	0.229

- (1) Classification based on Robertson (2010)
- (2) Classification based on Robertson (1990)
- (3) Calculated based on author's tailings CPT data and Equations 1 through 6
- (4) Calculated based on authors' tailings FVT data

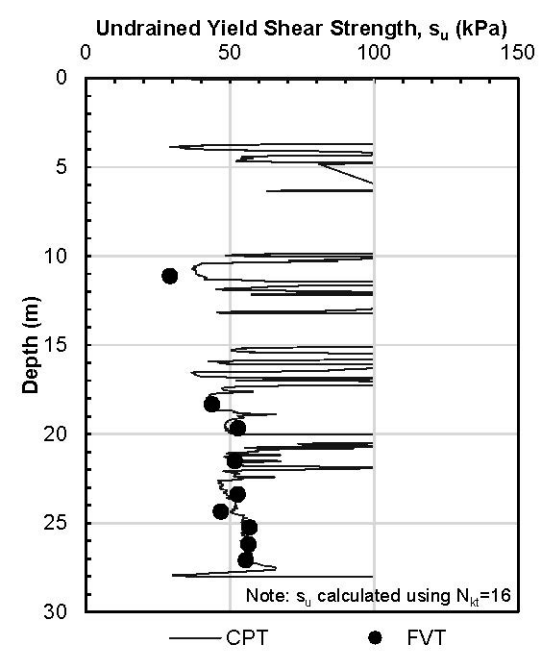


Figure 2. Tailings CPT and FVT profiles (case G from Table 3)

4.3 Susceptibility to liquefaction

Figure 3 presents the CPT data from the case history database (summarized in Table 2) and the CPT data from the authors' tailings dataset (summarized in Table 3) in terms of the normalized cone results with respect to the normalized CPT-based SBT chart. The normalized CPT-based SBT chart has lines delineating each SBT, as well as the contour line that represents a clean sand equivalent penetration resistance ($Q_{in,cs}$) of 70, proposed by Robertson (2010) to separates materials with contractive and dilative behavior in undrained shear. The mean value of the data presented in Figure 3 is represented by a square for the case histories and a circle for the authors' tailings dataset. The data from the author's tailings dataset include error bars to illustrate the variability (showing one standard deviation) of the normalized friction ratio, F_r , and normalized tip resistance, Q_m , at each location. It can be seen in Figure 3 that the mean values from the case histories are classified as SBT 3, 4, 5, and 6, and the mean values from the authors' tailings dataset are classified as SBT 3 with error bars extending into SBT 4. It can also be seen from Figure 3 that all of the data plot below Robertson's (2010) $Q_{in,cs}$ = 70 contour line, indicating contractive or strain softening behavior for the case histories and the authors' tailings dataset.

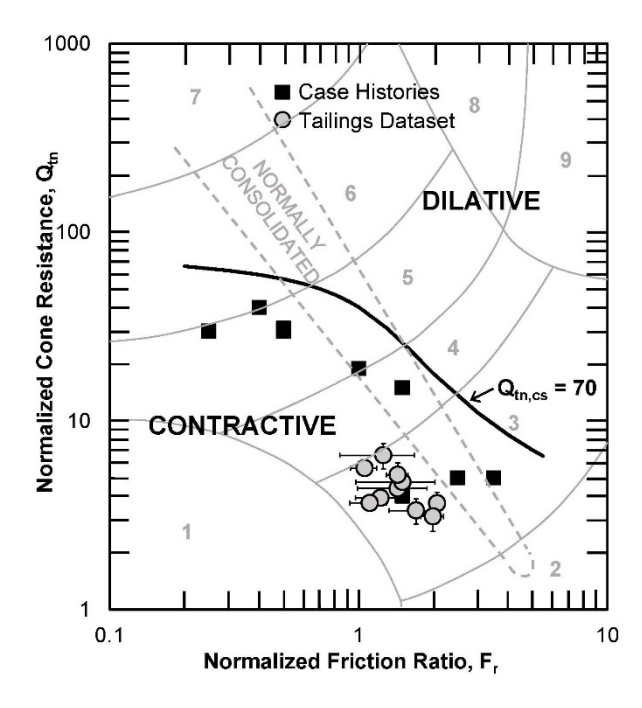


Figure 3. Soil behavior type (SBT) chart based on normalized CPT parameters (after Robertson 2010), showing Olson and Stark (2003) case histories and the author's tailings dataset

5 PRELIMINARY RELATIONSHIP BETWEEN $Q_{tn,cs}$ AND $S_{U \text{ (YIELD)}}/\sigma'_{VO}$

Based on the case histories and the authors' tailings dataset, the proposed relationship between $Q_{m,cs}$ and $s_{u \text{ (yield)}}/\sigma'_{vo}$ to use in liquefaction triggering analysis is shown in Figure 4. Figure 4 includes the mean value for each case history/location represented by squares for the case histories (Table 2) and circles for the authors' tailings dataset (Table 3). Figure 4 includes a linear regression trend line through the data points and also the linear trend line ± 1 standard deviation. This preliminary relationship between $Q_{m,cs}$ and $s_{u \text{ (yield)}}/\sigma'_{vo}$ can be represented by Equation 7:

$$s_{u \text{ (yield)}}/\sigma'_{vo} = 0.0015 (Q_{tn,cs}) + 0.1915 (\pm 0.043)$$
 (7)

Equation 7 was developed using materials with contractive behavior. Soils with a $Q_{tn,cs}$ greater than 70 are expected to be dilative and not susceptible to liquefaction, so the relationship between $Q_{tn,cs}$ and $s_{u \text{ (yield)}}/\sigma'_{vo}$ should not be used for $Q_{tn,cs}$ greater than 70.

It should be noted that not all data points fall within one standard deviation of the linear regression trend line represented by Equation 7. The three data points that fall above one standard deviation are not concerning; even though using the relationship would lead to under-prediction of the undrained yield shear strength ratio, this is conservative for use in liquefaction triggering analyses. The three data points that fall below one standard deviation are more concerning because using the relationship would over-predict undrained yield shear strength ratio.

To improve the preliminary relationship presented in Equation 7, additional data from a robust number of sites with variable tailings characteristics needs to be collected and analyzed. Additional data with a wider range of $Q_{tn,cs}$, s_{u} (yield)/ σ'_{vo} , and SBT should be collected and analyzed. Once the data set is expanded, the preliminary relationship can be revisited to assess if the trend between $Q_{tn,cs}$ and s_{u} (yield)/ σ'_{vo} can be refined and if it can be better represented by something other than a linear trend line. Lastly, the data presented in this paper can be further assessed to determine if there are reasons that can explain the scatter in the data.

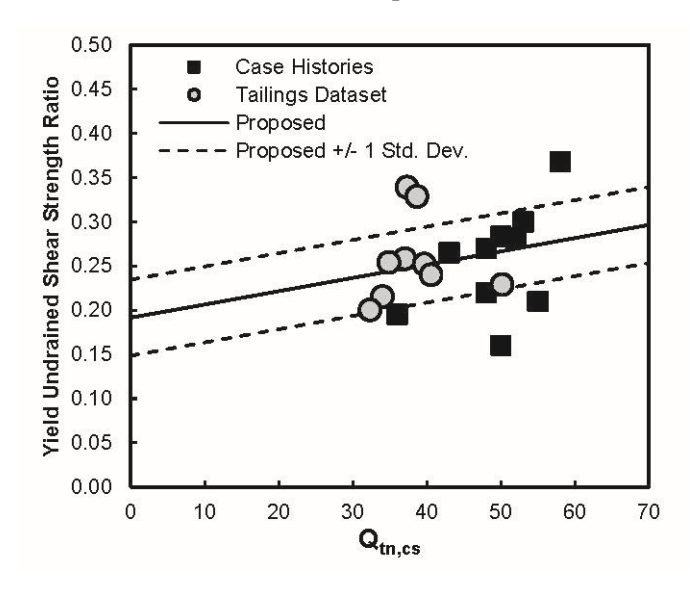


Figure 4. Relationship to predict yield undrained shear strength ratio based on $Q_{tn,cs}$ (linear regression ± 1 standard deviation)

6 SUMMARY AND CONCLUSIONS

A preliminary relationship for estimating the yield shear strength ratio, s_u (yield)/ σ'_{vo} , as a function of the equivalent clean sand cone penetration resistance, Q tn,cs, has been developed and presented. First, the CPT data from the case histories and the authors' tailings dataset were plotted on the normalized CPT-based SBT chart, which shows that all data used to develop the relationship plots below the $Q_{tn,cs}$ = 70 contour line. This indicates contractive or strain softening behavior. Then, the new relationship was developed by pairing $Q_{m,cs}$ from the case histories reported by Robertson (2010) with the corresponding yield strength ratio s_u (yield) σ'_{vo} from Olson and Stark (2003). Additional data from the authors, consisting of CPT and FVT soundings conducted in fine tailings, were included in the relationship development. The FVT allows for direct measurement of the yield shear strength, and the CPT data allows for the calculation of the normalized equivalent clean sand cone resistance, $Q_{tn,cs}$. Equation 7 is proposed on a preliminary basis as a relationship to estimate the yield shear strength ratio from $Q_{tn,cs}$, determined from CPT data for use in liquefaction triggering analysis. The authors intend to collect and analyze additional data to expand the dataset. The objective is to include a robust number of sites with variable tailings characteristics including $Q_{in,cs}$, s_{u} (yield)/ σ'_{vo} , and SBT to enhance the relationship and assess if a linear trend is the most appropriate for the data. The additional data, with an updated relationship for use over a broader range of conditions, will be published in the future.

ACKNOWLEDGEMENTS

The authors wish to thank Mr. Jason Harvey, Mr. Kurt Schimpke, and Mr. Richard Ver Strate of Barr Engineering Co. for their careful review of this paper and their continued work on the project. Additionally, they are grateful for the review and formatting provided by Ms. Annie

Breitenbucher of Barr Engineering Co. They also wish to thank their client for allowing data collected from their site to be used in this paper.

REFERENCES

- Blight, G. 1968. A Note on Field Vane Testing of Silt Soils. Canadian Geotechnical Journal 5(3): 142-149.
 Castro, G. 2003. Evaluation of seismic stability of tailings dams. Soil Rock America 2003. Proceedings of 12th Pan-American Conference on Soil Mechanics and Geotechnical Engineering. 39th U.S. Rock Mechanics Symposium, Cambridge, MA. July 2003.
- Contreras, I.A., Haggerty, M.B., and Schimpke, K.J. 2016. Observational Approach to Construction over Soft Tailings. *Proceedings of the 2016 Tailings and Mine Waste Conference*, Keystone, CO. October 2016:795–806.
- Davies, M.P., Dawson, B.B, and Chin, B.G. 1998. Static Liquefaction Slump of Mine Tailings A Case History. 51st Canadian Geotechnical Conference 1:123–131.
- Jefferies, M. and Been, K. 2006. Soil Liquefaction: A Critical State Approach, Second Edition. Boca Raton, FL: CRC Press.
- Kramer, S.L. and Wang, C.H. 2015. Empirical Model for Estimation of the Residual Strength of Liquefied Soil. *Journal of Geotechnical and Geoenvironmental Engineering* 141(9):04015038.
- Martin. T.E. and McRoberts, E.C. 1999. Some Considerations in the Stability Analysis of Upstream Tailings Dams. *Proceedings of the 6th International Conference on Tailings and Mine Waste* 287–302.
- Olson, S.M. 2001. Liquefaction Analysis of Level and Sloping Ground Using Field Case Histories and Penetration Resistance. PhD Thesis, University of Illinois at Urbana-Champaign.
- Olson, S.M. and Stark, T.D. 2003. Yield Strength Ratio and Liquefaction Analysis of Slopes and Embankments. *Journal of Geotechnical and Geoenvironmental Engineering* 129(8):727–737.
- Poulos, S.J., Castro, G., and France, W. 1985a. Liquefaction evaluation procedure. *Journal of Geotechnical Engineering* 111(6) 772–792.
- Poulos, S.J., Robinsky, E.I., and Keller, T.O. 1985b. Liquefaction resistance of thickened tailings. *Journal of Geotechnical Engineering* 111(12) 1380–1394.
- Poulos, S.J. 1988. Liquefaction and related phenomena. *Advanced dam engineering for design, construction, and rehabilitation*, R.B. Jansen, ed. Van Nostrand Reinhold, New York, 292–320.
- Robertson, P.K. 1990. Soil classification using the cone penetration test. *Canadian Geotechnical Journal* 27(1), 151–158.
- Robertson, P.K. 2010. Evaluation of Flow Liquefaction and Liquefied Strength Using the Cone Penetration Test. *Journal of Geotechnical and Geoenvironmental Engineering* 136(6):842–853.
- Sadrekarimi, A. 2014. Effect of the Mode of Shear on Static Liquefaction Analysis. *Journal of Geotechnical and Geoenvironmental Engineering* 140(12):04014069.
- Seed, H.B., et al. 1985. The influence of SPT procedures in soil liquefaction resistance evaluations. *Journal of Geotechnical Engineering* 111(12):1425–1445.
- Seed. H.B. and Harder, L.F. 1990. SPT-based analysis of cyclic pore pressure generation and undrained residual strength. *Proceedings of Seed Memorial Symposium*, BiTech Publishers, Vancouver, BC, Canada, 351–376.
- Shuttle, D.A. and Cunning, J. 2007. Liquefaction Potential of Silts from CPTu. *Canadian Geotechnical Journal* 44(1):1–19.
- Silvis, F. and de Groot, D. 1995. Flow slides in the Netherlands: Experience and engineering practice. *Canadian Geotechnical Journal* 32:1086–1092.
- Terzaghi, K., Peck, R., and Mesri, G. 1996. *Soil Mechanics in Engineering Practice*, Third Edition, New York, John Wiley and Sons.
- Youd, T.L. et al. 2001. Liquefaction resistance of soils: summary report from the 1996 NCEER and 1998 NCEER/NSF Workshops on evaluation of liquefaction resistance of soils. Journal of Geotechnical and Geoenvironmental Engineering, ASCE, 127(4):297–313.